Permanent Magnetism, Magnetic Anisotropy, and Hysteresis of Thiol-Capped Gold Nanoparticles

P. Crespo,[1] R. Litrán,[2] T. C. Rojas,[2] M. Multigner,[1] J. M. de la Fuente,[3] J. C. Sánchez-López,[2] M. A. García,[1] A. Hernando,[1] S. Penadés,[3] and A. Fernández[2,*]

[1]*Instituto de Magnetismo Aplicado (RENFE-UCM-CSIC), P.O. Box 155, 28230 Las Rozas, Madrid, Spain and Departamento de Física de Materiales, Universidad Complutense, Madrid, Spain*

[2]*Instituto de Ciencia de Materiales de Sevilla CSIC-USE, Américo Vespucio nr.49, 41092 Sevilla, Spain and Departamento de Quimica Inorgánica, Universidad de Sevilla, Spain*

[3]*Grupo Carbohidratos, Laboratory of Glyconanotechnology IIQ-CSIC, Américo Vespucio nr.49, 41092 Sevilla, Spain*

(Received 13 March 2004; published 20 August 2004)

We report on the experimental observation of magnetic hysteresis up to room temperature in thiol-capped Au nanoparticles with 1.4 nm size. The coercive field ranges from 860 Oe at 5 K to 250 Oe at 300 K. It is estimated that the Au atoms exhibit a magnetic moment of $\mu = 0.036\mu_B$. However, Au nanoparticles with similar size but stabilized by means of a surfactant, i.e., weak interaction between protective molecules and Au surface atoms, are diamagnetic, as bulk Au samples are. The apparent ferromagnetism is consequently associated with $5d$ localized holes generated through Au-S bonds. These holes give rise to localized magnetic moments that are frozen in due to the combination of the high spin-orbit coupling (1.5 eV) of gold and the symmetry reduction associated with two types of bonding: Au-Au and Au-S.

DOI: 10.1103/PhysRevLett.93.087204 PACS numbers: 75.75.+a, 73.22.–f, 75.30.Kz, 81.07.–b

Metallic nanoparticles (NPs) are extensively studied since they exhibit novel electronic, optical, and magnetic properties. Most of these new properties arise from the so-called "size effect" which affects the electronic structure, as well as from the increase of the ratio of atoms located at the surface with respect to the total number of atoms of the NP [1,2]. Monodispersed gold particles with an average size below 2 nm have been synthesized by different routes using ligands and surfactants as protective agents [3–5].

As is well known, XANES (x-ray absorption near-edge structure) measurements of bulk Au reveal features related to the existence of a small amount of itinerant holes at the d band caused by s-p-d levels hybridization. In Au NPs, a noticeable lattice contraction due to size effect has been observed and reported [6]. The decrease of Au interatomic distances yields enhancement of d-d electron interactions in such a way that the number of d holes decreases respect to that of bulk Au [2]. It has been also shown that in Au NPs capped with strong interacting thiols, the number of holes in the $5d$ band increases as indicated by the enhanced intensity of the white line feature, arising from $2p_{3/2,1/2} \rightarrow 5d$ dipole transition, in the XANES spectrum [7].

Therefore, in thiol-capped Au NPs the counterbalance between size effect and ligand effect tunes the structure and total number of d holes. Since magnetic behavior is determined by the d electrons, it is expected that the magnetic properties can be also tuned upon different capping and size. It should be remarked that nanosized particles holding permanent magnetic moment play a key role for the basic understanding of magnetism as well as for miniaturized data-storage technology [8]. An induced magnetic moment has been recently reported for gold at Au-Co interfaces [9], while in Ref. [10] (and references therein) the onset of ferromagnetism in Pd nanoparticles is discussed.

Calculations of the electronic structure for gold indicate that the d band lies well below the Fermi level where the density of states, $n(E_F) = 0.29\ \mathrm{eV}^{-1}\,\mathrm{atom}^{-1}$, is low enough [11] to promote noticeable Pauli paramagnetism. Consequently, the weak $5d$ band paramagnetism is overcome by the combination of Landau and core diamagnetism, and, as result, bulk gold is diamagnetic with a susceptibility of $\chi = -1.4 \times 10^{-7}\ \mathrm{emu/gOe}$ [12]. Nevertheless, in thiol-capped gold NPs, the extra holes induced in the $5d$ band by the thiol ligand are localized holes and, as will be shown below, give rise to an outstanding and very astonishing magnetic behavior.

In this work, Au NPs stabilized with different capping systems have been prepared by the chemical reduction of a metal salt precursor, in a liquid phase, in the presence of "protective" species that, due to the formation of covalent links or by electrostatic interactions, isolate the metal cluster preventing its growth. In the case of thiol-derivatized gold NPs, Au-SR, the preparation procedure is based on the Brust method [3], but this route has been modified by increasing the thiol:gold ratio to decrease the particle size average. R in this sample is a dodecane alkyl chain.

With the aim to compare the influence of the protective species on the structural, electronic, and magnetic behaviors of metal clusters, tetraalkylammonium ($R_4N^+X^-$) protected gold NPs with a weakly interacting dipole capping molecule have also been prepared [4]. In this case, the so-called Au-NR sample has been obtained

with tetraoctyl ammonium bromide as the surfactant molecule.

We combine the XANES with EXAFS (extended x-ray absorption fine structure) analysis to characterize gold NPs stabilized with the different capping systems. X-ray absorption spectra were recorded in fluorescence mode at the beam line BM29 in the ESRF storage ring in samples supported on cellulose filters. Magnetic characterization has been carried out with a SQUID magnetometer below 350 K. The contribution of the sample holder to the experimental magnetization, a diamagnetic one, has been substracted to obtain the NPs magnetization. The surface plasmon has been measured by means of UV-visible optical absorption spectroscopy.

Figure 1 shows the TEM micrographs and particle size distribution histograms for the capped gold NPs. Au-SR NPs present a narrow particle size distribution with an average size of 1.4 nm, whereas for sample Au-NR a bimodal distribution was observed centered at 1.5 and 5.0 nm.

Figure 2 shows the XANES spectra of the Au-L_3 edge for the two different capped NPs and for bulk Au. According to the area under the white line [7], shown in Fig. 2, the charge transfer from gold to sulfur atoms is extremely large in the Au-SR sample. In addition to that, the inset of Fig. 2 shows the Fourier transform (FT) of the L_3-edge EXAFS oscillations for both samples as compared to bulk gold. For the Au-SR sample, Au-Au and Au-S coordination numbers of 2.0 and 1.3 were, respectively, found after EXAFS fitting procedure. This value is also in agreement with the S:Au atomic ratio of 1.0 evaluated by energy-dispersive x-ray (EDX) analysis.

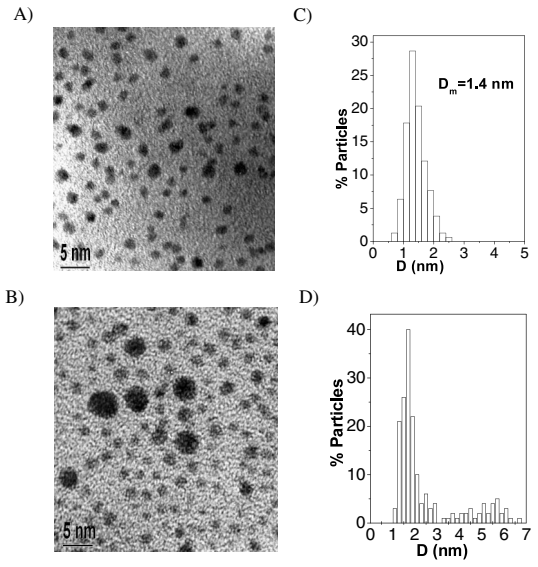

FIG. 1. Transmission electron micrographs of Au-SR (a) and Au-NR (b) NPs. Their corresponding histograms, obtained from several micrographs, are plotted, respectively, in (c) and (d).

For a 1.4 nm size pure gold particle, we estimate a total number of atoms of 79, where 75% percent of them are located at the surface. If we consider one sulfur atom bound to one surface gold atom, we expect Au-S coordination numbers of 0.75. The increase in this coordination number, according to EXAFS and EDX, could be explained by assuming a multiple Au-S bond at surface gold atoms or, more likely, to the formation of a depletion shell in the nanoparticles where excess sulfur is present, as illustrated in the inset of Fig. 2. This last hypothesis also explains the very small Au-Au coordination numbers and the important increase in the *d*-hole density. Besides that, the Au-Au bond length evaluated by EXAFS fitting analysis for the Au-SR sample has been estimated to be 2.98 Å, which is 5% larger than the corresponding value for bulk gold, 2.83 Å. This expansion of the very small Au-Au core cluster indicates that charge transfer to the capping molecule is overcoming nanosize effects that tend to contract the Au lattice [6]. For the alkyl ammonium protected NPs (Au-NR sample), the Au-Au bond length estimated from the Fourier transform of the EXAFS oscillations is 2.84 Å, which is compatible with a weak interacting dipole capping molecule and the observed particle size distribution histogram.

Figure 3 shows the hysteresis loops measured at 5 and 300 K for Au-NR and Au-SR samples. NPs dispersed by a surfactant (Au-NR sample) exhibit a diamagnetic behavior, similar to that of bulk gold. In these particles, the density of 5*d* holes, as measured by XANES, is similar to the one from bulk gold, and the electrons and holes of the 5*d* band are itinerant as evidenced by the observed resonance in the UV-visible absorption spectrum in Fig. 4. This band is associated to the so-called surface plasmon resonance [13], which corresponds to a collective oscillation of electrons inside the NP. In the case of gold, the largely polarizable 5*d* electrons are the main contributors

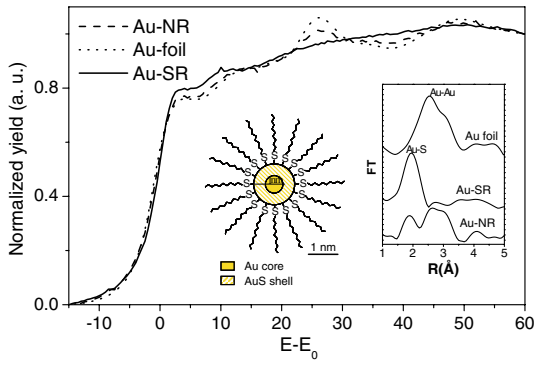

FIG. 2 (color online). Au-L_3-edge XANES spectra for the two different gold NPs compared to bulk gold. The insets show the modulus of the Fourier transform at the Au-L_3 edge (*K* weighted, *k* space range of 3–12 Å without phase correction) for both samples and a schema of the proposed structure for Au-SR.

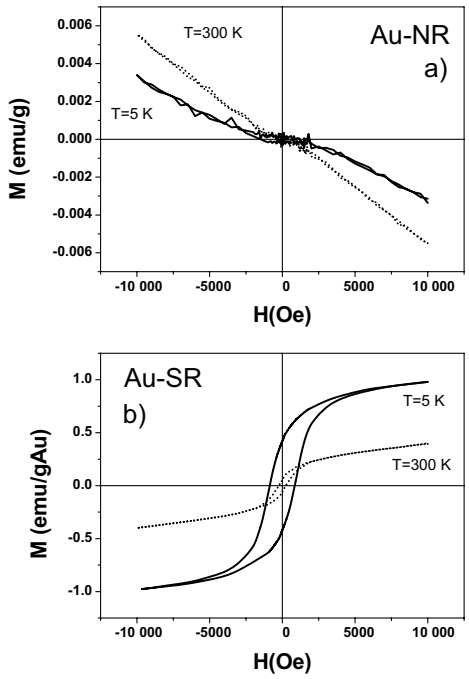

FIG. 3. Magnetization curves of gold nanoparticles stabilized by means of a surfactant, Au-NR (a), and hysteresis loops corresponding to the gold thiol-capped NPs, Au-SR (b), at 5 and 300 K. For the Au-SR sample, the magnetization is given in emu per gram of gold.

to this absorption. The shape of the measured absorption curve is characteristic of isolated NPs [13], without aggregation effects. The surface plasmon resonance is, however, absent for the Au-SR sample, suggesting that due to the effect of Au:S bonding the $5d$ electrons of the gold NP have lost itinerancy and behave as localized or partially localized carriers.

It is evident from Fig. 3 that the magnetization process of thiol-capped gold NPs (Au-SR sample) proceeds similarly to typical ferromagnetic materials describing a hysteresis loop even up to room temperature. Notice the high values of the coercive field, 860 Oe at 5 K that decreases down to 250 Oe at room temperature. In addition, it is observed that the samples are not saturated at any temperature. Remanence values around half of the magnetization value reached at 1 T are measured. This remanent magnetization implies that, under an applied field, the NPs system behaves as an assembly of magnetic moments randomly distributed in orientation [14].

It may be argued that the observed behavior is due to the presence of ferromagnetic impurities. Inductive coupled plasma analysis indicates that the amount of Fe impurities (of the order of 0.007 wt%) is too low to account for the obtained magnetization values.

Since gold NPs dispersed by a surfactant (Au-NR) are diamagnetic, the apparent ferromagnetism observed in Fig. 3 for Au-SR samples must be associated with the modification introduced in the Au electronic structure by the Au:S bond. The main modification consists of the induction of $5d$ band holes localized in the vicinity of the thiol bond and the subsequent lattice expansion with respect to bulk Au. Therefore, the permanent magnetic moment of an Au atom bound to an S atom can be estimated, from the spin associated to the localized hole, as the Bohr magneton times the atomic charge transfer due to bonding. From the value of the magnetization for sample Au-SR at 5 K under an applied field of 1 T, an estimation of the lower limit value (since the samples are not saturated) of the magnetic moment of gold atoms is straightforward. The value of the magnetic moment per Au atom bound to sulfur (practically all the gold atoms in the particle) is estimated as to be $\mu_{\mathrm{at}} = 0.036\mu_B$, μ_B being the Bohr magneton. This indicates a d-charge loss of around $\approx 0.036\ e$/atom, which is in very good agreement with a calculated value of $\approx 0.05\ e$/atom charge transfer in $Au_{38}(SCH_3)_{24}$ [15] and with the value of $\approx 0.07\ e$/atom obtained through XANES studies on thiol-capped Au NPs [7,16].

The most exciting and intriguing feature of the Au-SR sample is the hysteresis observed up to room temperature indicating that the blocking temperature is above 300 K, which for this particle size requires a value of the anisotropy constant, k, higher than 7×10^7 J/m^3 or 10 meV/atom. Such an enormous value, larger than that corresponding to typical systems with high anisotropy such as hexagonal $SmCo_5$ ($k = 1.2$ meV/Co atom), becomes reasonable after considering the high strength of the spin-orbit coupling for gold, 1.5 eV [16,17]. In fact, the intrinsic magnetic anisotropy appears from the balance between the spin-orbit coupling and the lack of spherical symmetry in the distribution of the electric charges surrounding the magnetic atom. As stated from the previous described microstructural study, in our case the Au magnetic atoms undergo Au-Au and Au-S types of

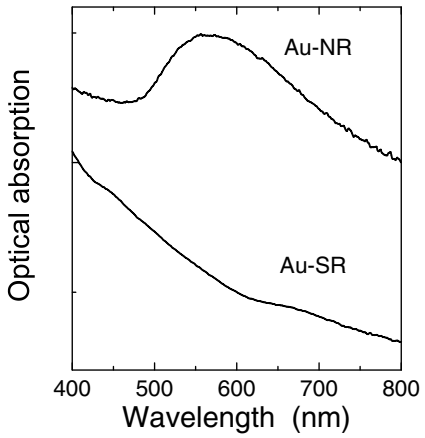

FIG. 4. UV-visible absorption spectra for the two studied gold nanoparticles. The strong surface plasmon resonance band around 550 nm, observed for the Au-NR sample, is absent in the case of Au-SR.

bonding, which give rise to a lack of spherical symmetry of the neighbor electric charge distribution. A similar argument has been recently proposed by Gambardella *et al.* [18] to account for giant magnetic anisotropy of isolated Co atoms and NPs deposited onto single crystal Pt substrates.

It is important to remark that the experimental hysteresis shown in Fig. 3 points out the existence of a combination of permanent magnetic moments and high magnetic anisotropy but do not imply the presence of large exchange interactions. For very small particles with p local magnetic moments, of strength μ, randomly distributed in orientation, the expected resultant moment per particle is $p^{0.5}\mu$, whereas it would have been $p\mu$ for a ferromagnetic configuration. It is obvious that for low p values the overall moment of the NP inferred from remanence measurements is of the same order for both configurations. Therefore, the appearance of frozen in permanent magnetic moments in a NP can be understood, without necessarily invoking a ferromagnetic configuration. Even though intraparticle direct exchange interactions between localized moments are not necessarily inferred from the experimental results, its possible influence should not be discarded.

The orientation of the local easy axis (or axes) of the magnetic moment at any Au atomic site should be whatever (in plane or out plane) but determined by the direction of the Au-S bond. Accordingly, we suggest that the NPs likely behave as a random anisotropy system. The enormous strength of the spin-orbit coupling for Au, 1.5 eV, and the consequent giant magnetic anisotropy, 10 meV/atom, presumably overcomes exchange effects.

As the NPs are dispersed, interparticle interactions can be only of magnetostatic nature. The average distance between gold NPs is determined by the length of the thiol-alkyl chain (1.7 nm). This distance will be around 3.3 nm for the Au-SR sample, assuming no interpenetration of alkyl chains, and it will take a minimum possible value of 1.7 nm. As the permanent magnetic moment of each particle is very low, approximately of 1.5 Bohr magnetons, the magnetic field acting on a NP due to a single neighbor NP is lower than 10 Oe; therefore the influence of the stray fields can be neglected. The lack of considerable interparticle interactions is also supported by the structureless plasmon resonance curve of the Au-SR sample.

In conclusion, it has been shown (Fig. 3) that very small thiol-capped gold NPs exhibit a localized permanent magnetism in contrast to the metallic diamagnetism characteristic of Au-NR sample or bulk Au. This observation points out that thiol-bonding induces in Au NPs not only hole localization and lattice expansion, which tends to mask the contraction induced by size effects, but also permanent magnetic moments associated with the spin of extra d holes localized near the Au-S bonds. We suggest that the strong spin-orbit coupling of Au, associated with a high local anisotropy, freezes the magnetic moments along the local easy axis and gives rise to the appearance of permanent magnetism at NP scale.

XAS facilities at BM29 in ESRF and the technical support from O. Mathon are acknowledged. The authors thank J. Llopis and I. Rosa for helping with optical measurements and sample preparation, respectively. Financial support from the Spanish MCyT under Projects No. MAT2002-04246-C05-05 and No. BQU2002-03734 is acknowledged.

*Corresponding author.
Electronic address: asuncion@icmse.csic.es

[1] A. P. Alivisatos, Science **271**, 933 (1996).
[2] I. Coulthard, I. S. Degen, Y. Zhu, and T. K. Sham, Can. J. Phys. **76**, 1707 (1998).
[3] M. Brust, M. Walker, D. Bethell, D. J. Schiffrin, and R. Whyman, J. Chem. Soc. Chem. Commun. **1994**, 801 (1994).
[4] M. T. Reetz and M. Maase, Adv. Mater. **11**, 773 (1999).
[5] J. M. de la Fuente, A. G. Barrientos, T. C. Rojas, J. Rojo, J. Cañada, A. Fernández, and S. Penadés, Angew. Chem., Int. Ed. Engl. **40**, 2257 (2001).
[6] D. Zhanchet, H. Tolentino, M. C. Martin Alves, O. L. Alves, and D. Ugarte, Chem. Phys. Lett. **323**, 167 (2000).
[7] P. Zhang and T. K. Sham, Appl. Phys. Lett. **81**, 736 (2002); P. Zhang and T. K. Sham, Appl. Phys. Lett. **81**, 736 (2002); I. L. Garzón, C. Rovira, K. Michaelian, M. R. Beltrán, P. Ordejon, J. Junquera, D. Sánchez-Portal, E. Artacho, and J. M. Soler, Phys. Rev. Lett. **85**, 5250 (2000).
[8] Special Issue on Magnetism, edited by M. R. Ibarra [Europhysics News **34**, 209 (2003)].
[9] F. Wilhelm, M. Angelakeris, N. Jaouen, P. Poulopoulos, E. Th. Papaioannou, Ch. Mueller, P. Fumagalli, A. Rogalev, and N. K. Flevaris, Phys. Rev. B **69**, 220404(R) (2004).
[10] B. Sampedro, P. Crespo, A. Hernando, R. Litrán, J. C. Sánchez-López, C. López Cartés, A. Fernández, J. Ramírez, J. González Calbet, and M. Vallet, Phys. Rev. Lett. **91**, 237203 (2003).
[11] D. A. Papaconstantopoulous, *Handbook of Band Structure of Elemental Solids* (Plenum Press, New York, 1986).
[12] E. Vogt, *Magnetism and Metallurgy I*, edited by A. E. Berkowitz and E. Kneller (Academic Press, New York, 1969), p. 252.
[13] U. Kreibig and M. Völlmer, *Optical Properties of Metal Clusters* (Springer-Verlag, Berlin, 1995).
[14] E. C. Stoner and E. P. Wohlfarth, Philos. Trans. R. Soc. London A **240**, 599 (1948).
[15] H. Hakkinen, R. Barnett, and U. Landman, Phys. Rev. Lett. **82**, 3264 (1999).
[16] P. Zhang and T. K. Sham, Phys. Rev. Lett. **90**, 245501 (2003).
[17] R. Skomski and J. M. D. Coey, *Permanent Magnetism* (Institute of Physics Publishing, Bristol, 1999), Chap. 3.
[18] P. Gambardella *et al.*, Science **300**, 1130 (2003).